Applied and Environmental Microbiology, Nov. 2010, p. 7598–7607 Vol. 76, No. 22
0099-2240/10/$12.00 doi:10.1128/AEM.00312-10

Changes in Ultrastructure and Fourier Transform Infrared Spectrum of *Salmonella enterica* Serovar Typhimurium Cells after Exposure to Stress Conditions[▽]

A. Alvarez-Ordóñez and M. Prieto*

Department of Food Hygiene and Technology, Veterinary Faculty, University of León, 24071 León, Spain

Received 4 February 2010/Accepted 8 September 2010

The effect of exposure to acid (pH 2.5), alkaline (pH 11.0), heat (55°C), and oxidative (40 mM H_2O_2) lethal conditions on the ultrastructure and global chemical composition of *Salmonella enterica* serovar Typhimurium CECT 443 cells was studied using transmission electron microscopy and Fourier transform infrared spectroscopy (FT-IR) combined with multivariate statistical methods (hierarchical cluster analysis and factor analysis). Infrared spectra exhibited marked differences in the five spectral regions for all conditions tested compared to those of nontreated control cells, which suggests the existence of a complex bacterial stress response in which modifications in a wide variety of cellular compounds are involved. The visible spectral changes observed in all of the spectral regions, together with ultrastructural changes observed by transmission electron microscopy and data obtained from membrane integrity tests, indicate the existence of membrane damage or alterations in membrane composition after heat, acid, alkaline, and oxidative treatments. Results obtained in this study indicate the potential of FT-IR spectroscopy to discriminate between intact and injured bacterial cells and between treatment technologies, and they show the adequacy of this technique to study the molecular aspects of bacterial stress response.

Salmonella spp. are an important cause of bacterial food-borne disease all over the world, causing a diversity of illnesses that include typhoid fever, gastroenteritis, and septicemia (11). According to epidemiological data from the European Union, a total of 131,468 laboratory-confirmed salmonellosis cases were reported in 2008, with two serovars, *Salmonella enterica* serovar Typhimurium and *Salmonella enterica* serovar Enteritidis, being responsible for 79.9% of all cases (13). The detection and identification of pathogens in foods are a basic cornerstone of food safety, because they make it possible to identify sources of contamination, provide data on the evaluation of risk reduction measures, and identify the food chain operations, processes, batches, or products representing a threat to public health. Furthermore, they also are fundamental in the epidemiological investigation of food-borne diseases. The presence of stress-injured bacterial cells in foods represents a challenge to those involved in food quality assurance, as routine microbiological procedures may yield negative results for sublethally injured cells. Thus, food could be presumed to be safe and free from pathogenic cells but during storage become dangerous due to the recovery and growth of previously injured cells.

Given the fact that bacterial cells react to the different environmental stress conditions by inducing structural and physiological changes, Fourier transform infrared (FT-IR) spectroscopy, which reflects the biochemical composition of the cellular constituents of bacteria that include water, fatty acids, proteins, polysaccharides, and nucleic acids (26), should be able to monitor the changes occurring in bacterial cells in response to several food-related stress conditions. The potential of this methodology to detect and differentiate sublethally heat-injured and dead *Listeria monocytogenes* and *S.* Typhimurium cells and to discriminate between diverse heat treatment intensities has been highlighted (2, 20). FT-IR spectroscopy also has been successfully applied to the identification and classification of bacteria such as *Acinetobacter* (35), *Brucella* (23), *Campylobacter* (24, 25), *Escherichia coli* (1), *Lactobacillus* (10, 27), *Listeria* (28, 29), *Salmonella* (9, 17), *Staphylococcus* (8, 19), and *Yersinia* (18).

The main aim of this study was to assess ultrastructural modifications and infrared (IR) spectral changes at different degrees of stress exposure and to discriminate between injured and noninjured *S.* Typhimurium cells after their exposure to heat, acid, alkaline, and oxidative lethal conditions. Results obtained also could help us improve our knowledge of *S.* Typhimurium cell damage and strategies of response to these adverse conditions.

MATERIALS AND METHODS

Bacterial strain and culture conditions. The *Salmonella enterica* serovar Typhimurium strain CECT 443 used in this study was obtained from the Spanish Type Culture Collection (Colección Española de Cultivos Tipo [CECT]). The lyophilized cultures were resuscitated in brain heart infusion (BHI; Oxoid) and incubated for 24 h at 37°C. Pure cultures were maintained on BHI agar (BHIA; Oxoid) plates at 4°C. Precultures were prepared by transferring an isolated colony from a plate into a test tube containing 10 ml of sterile BHI followed by incubation at 37°C for 24 h. Flasks containing 50 ml of sterile BHI then were inoculated with the preculture to a final cellular concentration of 10^3 cells/ml, and these cultures were incubated at 37°C for 24 h (the time at which cells are in a late stationary phase of growth) and then were used to determine the bacterial resistance to heat, acid, alkaline, and oxidative stresses and to perform the FT-IR spectroscopy measurements.

Assessment of heat, acid, alkaline, and oxidative resistance. Cell cultures were harvested by centrifugation at 8,000 × *g* for 5 min at 4°C (Eppendorf centrifuge

* Corresponding author. Mailing address: Department of Food Hygiene and Technology, Veterinary Faculty, University of León, 24071 León, Spain. Phone: 34 987 291 283. Fax: 34 987 291 284. E-mail: miguel.prieto@unileon.es.

▽ Published ahead of print on 17 September 2010.

5804R). The supernatant liquid was discarded, cells were resuspended in 10 ml of phosphate-buffered saline (PBS, Sigma Aldrich), and, afterwards, survival was monitored after exposure to (i) 55°C, (ii) pH 2.5 with 1 N HCl (Panreac), (iii) pH 11.0 with 1 N NaOH (Panreac), and (iv) H_2O_2 at 40 mM (Panreac). Tenfold serial dilutions were produced in sterile 0.1% (wt/vol) peptone solution (Oxoid), and suitable dilutions were plated in duplicate on BHIA. Viable cell densities at several points in time were enumerated following the incubation of the plates at 37°C for 48 h (longer incubation times did not have any influence on the count). Three different freshly grown cultures were used for each experimental run.

To fit the survival curves obtained, the following mathematical function based on the Weibull distribution was used: $\log N_t/N_0 = -(t/\delta)^p$, where t is the treatment time, N_t and N_0 are the population densities (CFU/ml) at time t and time zero, respectively, and δ and p are the scale and shape parameters, respectively.

The δ value represents the time needed to inactivate the first log cycle of the population. The p parameter accounts for the upward concavity of a survival curve ($p < 1$), a linear survival curve ($p = 1$), and downward concavity ($p > 1$) (21, 34). To determine the δ and p values, the least-squares criterion by GraphPad PRISM (GraphPad Software) was used.

Obtention of FT-IR profiles. Control cells, resuspended in PBS as described above, and cells subjected to heat (55°C), acid (pH 2.5), alkaline (pH 11.0), and oxidative (H_2O_2 at 40 mM) conditions at different points in time were harvested by centrifugation at 8,000 × *g* for 5 min at 4°C and suspended in 100 μl of PBS, placed (10 μl) in a ZnSe window, and stove dried (15 min, 50°C). Infrared spectra were obtained with an FT-IR spectroscope (Perkin-Elmer system 2000 FT-IR) equipped with a DTGS detector. Measurements were recorded over the wavelength range of 3,500 to 700 cm^{-1}, with an interval of 1 cm^{-1}. The spectral resolution was 4 cm^{-1}. The final spectra of the samples were achieved averaging 20 scans. Digitized IR spectra (with a total of 2,800 points) were saved and mathematically processed.

To obtain reproducible data, a strict experimental protocol was established in relation to medium preparation, incubation time and temperature, cell harvesting conditions, sample preparation and FT-IR measurement. Therefore, experimental conditions (see below) as well as the measuring time and resolution were standardized for each FT-IR measurement. The FT-IR experiments were conducted in triplicate using three different fresh cultures and with three separate measurements for each experimental run (nine different spectra for each strain exposure).

Transformation of spectra. A software application developed for the Perkin-Elmer environment was used for transformation, including normalization (0 setting with absorption at 1,800 cm^{-1}; 1 setting at maximal absorption, located around 1,650 cm^{-1}), smoothing, and second derivative (Savitzky-Golay algorithm). After transformation, spectra were recorded in ASCII format and processed (22, 24). The whole spectrum was divided for calculation purposes into five spectral windows (26): the window between 3,000 and 2,800 cm^{-1}, influenced by functional groups of membrane fatty acids (w_1); the window between 1,800 and 1,500 cm^{-1}, affected by amide I and amide II groups belonging to proteins and peptides (w_2); the window between 1,500 and 1,200 cm^{-1}, mixed region influenced by proteins, fatty acids and phosphate-carrying compounds (w_3); the window between 1,200 and 900 cm^{-1}, which is informative mostly for the carbohydrates and polysaccharides in the cell wall (w_4); and the window between 900 and 700 cm^{-1}, named the true fingerprint because of very specific spectral patterns characteristic at the species level (w_5).

Spectral reproducibility and grouping. To study variability between replicates and within windows, samples were processed in independent experiments, yielding nine replicates for each treatment condition. Pearson's correlation coefficient was calculated for the whole IR working range (3,000 to 2,800 and 1,800 to 700 cm^{-1}) and independently for the ranges described (w_1 to w_5). The mean of the correlation coefficients (r_1 to r_9) included in the correlation matrix was calculated, considering the nine replicates for each treatment. The spectral data were subjected to multivariate statistical methods (hierarchical cluster analysis [HCA] and factor analysis [FA]) to separate spectra into different classes. As an unsupervised classification method, HCA depicts similarity relationships between IR spectra without aprioristic knowledge about the samples studied. For FT-IR data, a final HCA was done on spectra belonging to the exposed samples (average of the nine replicates). Pearson's product moment correlation coefficient was used to measure the similarity between spectra, and strain clustering was achieved using Ward's algorithm. In addition to HCA, FA was performed on the same derivatized spectra. FA is a multivariate procedure that is used mainly to reduce the dimensionality of a data set and to detect structure in the relationships between variables. A set of correlated variables thus is transformed to a set of uncorrelated, hidden variables (factors) ranked by variability in descending order. All of the analyses (calculation of coefficients, joining of variables, canonical analysis, and graphical display) were carried out with the Statistica for Windows, v. 7.0, program (Statsoft Inc.).

Transmission electron microscopy. *S.* Typhimurium cells treated for the time needed for each stress condition to inactivate the first log cycle of the population (δ value) were harvested by centrifugation and fixed in 2.5% glutaraldehyde (TAAB Laboratories)–PBS for 3 h at 4°C. Bacteria then were washed in PBS for 30 min, and this washing step was repeated twice. Afterwards, cells were treated with osmium tetroxide (TAAB Laboratories)–1% PBS for 45 min at room temperature in darkness, followed by three new washing steps. Cells were pelleted in bacteriological agar (Oxoid), and the pellets subsequently were dehydrated in ethanol solutions of increasing concentration and embedded in an epoxy resin (Epon 812; Tousimis), which was polarized by incubation for 48 h at 60°C. Ultrathin sections were collected onto copper grids and stained with uranyl and lead. Observations were made using a JEOL 1010 microscope at 80 kV.

Measurement of cellular leakage. Aliquots of 3 ml of cell cultures treated at (i) 55°C, (ii) pH 2.5 with 1 N HCl, (iii) pH 11.0 with 1 N NaOH, and (iv) H_2O_2 at 40 mM for several time periods were filtered through a 25-mm-diameter, 0.22-μm-pore-size Millex-GS syringe filter (Millex-GS). The presence of nucleic acids and proteins in the filtrate was checked by measuring the absorbance at 260 and 280 nm, respectively (Uvikon 810 spectrophotometer).

Sorting of viable cells after heat treatment. To assess the viable status of *S.* Typhimurium heat-stressed cells, the *Bac*Light Redox Sensor Green Vitality kit (Molecular Probes, Invitrogen) was used. *S.* Typhimurium cultures grown until stationary phase were treated at 55°C for 12 min and subsequently diluted in PBS to ~10^7 cells/ml. Afterwards, 1 μl of Redox Sensor Green reagent (1 mM solution in dimethylsulfoxide [DMSO]) was added to 1 ml of the bacterial suspension. This reagent penetrates both Gram-positive and Gram-negative bacteria and is used as an indicator of bacterial reductase activity. To assess cell membrane integrity, 1 μl of propidium iodide was added and the mix was incubated in the dark at room temperature for 10 min. Prior to the analysis of the sample by flow cytometry, the cell suspension was centrifuged at 11,000 × *g* at 4°C for 5 min, and the pellet was suspended in PBS. A flow cytometer, a Coulter Epics Altra (Beckman Coulter, Inc.), was used for the sorting of viable *S.* Typhimurium cells. Optical filters were used to measure the green fluorescence of Redox Green sensor at 530 nm (PMT2) and the red fluorescence of propidium iodide at 575 nm (PMT3). Signals were discriminated based on their peak forward scatter signal and sorted based on a region of interest around their light scatter cluster, together with green-only fluorescence.

RESULTS

To determine the influence of several lethal stress conditions on the FT-IR spectra of *S.* Typhimurium CECT 443, stationary-phase cells grown in BHI were treated at (i) 55°C, (ii) pH 2.5 with 1 N HCl, (iii) pH 11.0 with 1 N NaOH, and (iv) H_2O_2 at 40 mM, and IR spectra were measured with an FT-IR spectroscope. Figure 1 shows the survival curves obtained as well as untransformed representative FT-IR spectra of treated samples at various points in time. Whereas survival curves obtained for acid-, alkaline-, and oxidative stress-treated cells were well described using a linear model (data not shown), survival curves obtained after the heat treatment were concave upward, which indicates a rapid bacterial inactivation during the first moments of exposure and a slow decrease of the number of survivors as the treatment time increases. For this reason, a nonlinear model based on the Weibull distribution was used to analyze and compare all survival curves obtained. In terms of R^2 (≥0.95; data not shown) and root mean square error (RMSE) (≤0.39; data not shown), this model accurately described the kinetics of inactivation. The estimated inactivation parameters, p (shape parameter which accounts for upward concavity [$p < 1$], a linear survival curve [$p = 1$], and downward concavity [$p > 1$]) and δ (scale parameter that represents the time needed to inactivate the first $\log_{10}$ cycle of the population), are shown in Table 1.

The spectrum of *S.* Typhimurium nontreated (control) cells was visually similar to the spectra reported in previous studies

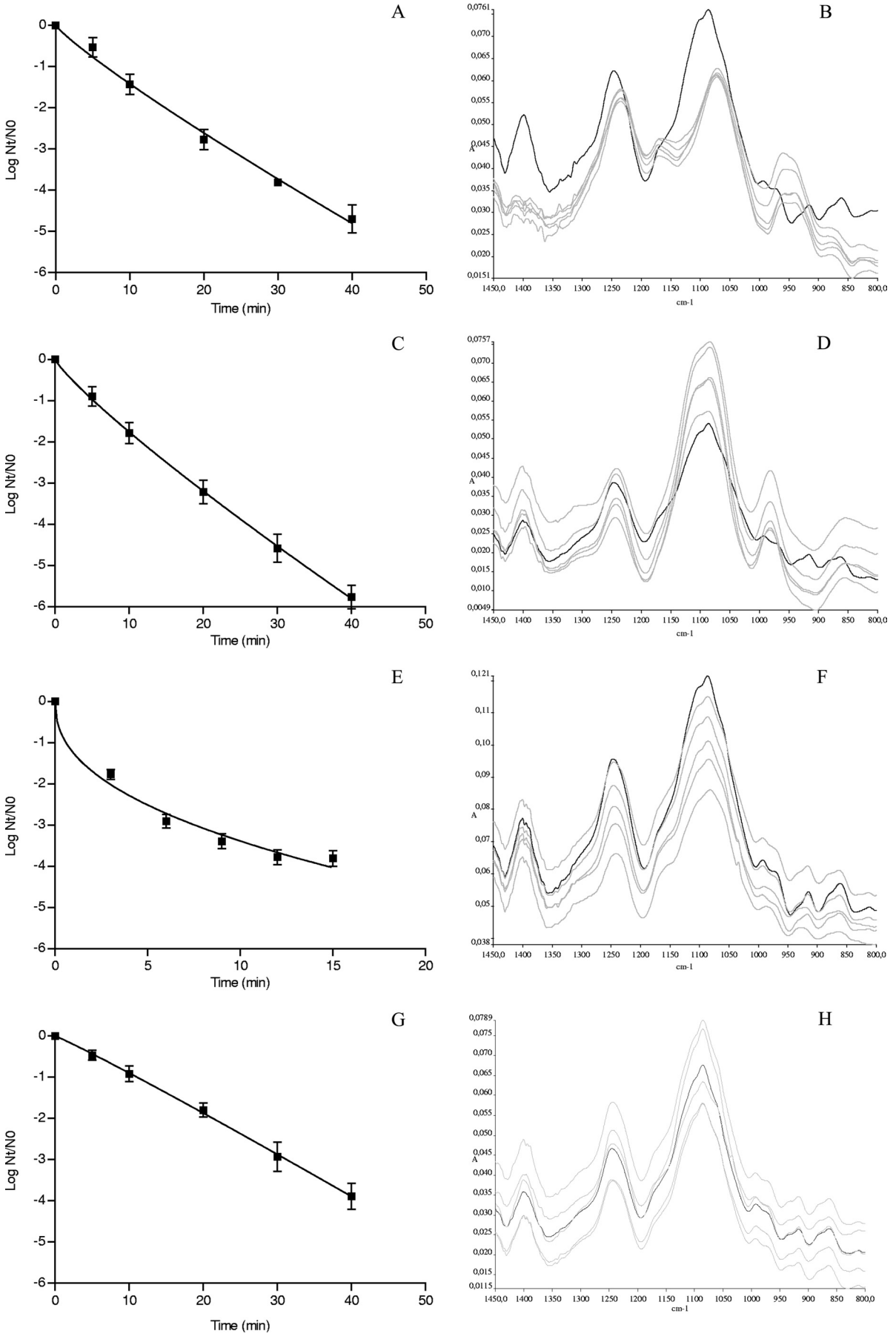
A
Log Nt/N0
Time (min)
B
A
cm-1
C
Log Nt/N0
Time (min)
D
A
cm-1
E
Log Nt/N0
Time (min)
F
A
cm-1
G
Log Nt/N0
Time (min)
H
A
cm-1

TABLE 1. Estimated δ and *p* values for *S.* Typhimurium CECT 443 heat-, acid-, alkaline-, and oxidative stress-treated cells[a]

Treatment condition	δ (min)	*p*
Heat (55°C)	0.59 ± 0.20	0.43 ± 0.05
Acid (pH 2.5)	6.72 ± 0.91	0.88 ± 0.08
Alkaline (pH 11.0)	5.18 ± 0.73	0.86 ± 0.07
Oxidation (H_2O_2 at 40 mM)	11.05 ± 1.06	1.06 ± 0.11

[a] δ and *p* values were estimated from the fit of the mathematical model log $N_t/N_0 = -(t/\delta)^p$ to experimental data of *S.* Typhimurium CECT 443 heat (55°C)-, acid (pH 2.5)-, alkaline (pH 11.0)-, and oxidative stress (H_2O_2 at 40 mM)-treated cells.

for *Salmonella* spp. and other bacteria (2, 7, 9, 12, 17, 26). Strong absorptions were detected in the five spectral regions (w_1, w_2, w_3, w_4, and w_5) that characterize the major cellular constituents. It is worth noting that whereas apparently similar FT-IR spectra were observed for cells exposed to heat and oxidative stress, the spectra obtained for acid- and alkaline-treated samples showed visible changes, even without any spectral transformation, especially in w_3 and w_4 regions (Fig. 1). Acid-treated cells showed important variations in the shape and intensity of several spectral bands. Thus, a reduction in the intensity of the peak found at approximately 1,400 cm^{-1}, which seems to be composed of two separate new bands, at 1,411 and 1,385 cm^{-1}, was observed, new peaks emerged at 1,171 cm^{-1} and 936 to 962 cm^{-1}, and the band found at 1,084 cm^{-1} was less intense and was found at approximately 1,074 cm^{-1}. On the other hand, a new band at 979 cm^{-1} and visible changes in the range of 915 to 858 cm^{-1} were found for alkaline-treated samples. All of these significant changes already were obvious at short treatment times, at which a large proportion of the bacterial population still remains viable, and apparently did not progress throughout the treatment. The spectra were further processed with the aim of minimizing methodological variability and amplifying the chemically based spectral differences. The normalization of the spectra balanced the differences in path strength, smoothing eliminated the instrumental noise, and the conversion of the spectra to their second derivative separated absorption bands, removed baseline shifts, and increased spectral resolution. This sort of signal transformation made differences between spectral features of treated and nontreated cells much more prominent.

The reproducibility of spectra was measured for the whole working range (3,000 to 2,800 and 1,800 to 700 cm^{-1}) and separately for the five spectral ranges described above by using the Pearson coefficient, using the means of the correlation triangle matrix (data not shown). Although in all cases there existed low variability among replicates (Pearson coefficient of >0.91), the spectral windows w_1 (mean Pearson coefficient of 0.99) and w_4 (mean Pearson coefficient of 0.98) showed the highest reproducibility.

The hierarchical classification of the second derivative spectra revealed differences among all phenotypes tested (including nontreated control cells) for the five spectral regions, although the region w_4, with a linkage distance of 3.8, was the most discriminant region (Fig. 2). An FA of this spectral region allowed us to discriminate between four main groups of samples (Fig. 3): the first including nontreated, oxidative stress-treated, and short-time heat-treated (3 and 6 min) samples (C1), the second including long-time heat-treated (9, 12 and 15 min) samples (C2), the third including alkaline-treated samples (C3), and the fourth from acid-treated samples (C4), with the latter group showing the most remarkable spectral changes. It is worth noting that, whereas for heat-treated cells a gradual effect of treatment time was observed, spectral modifications observed for alkaline- and acid-treated samples were detected immediately after exposure. Interestingly enough, oxidative stress did not significantly affect the IR spectrum. Qualitatively similar results were obtained for w_1, w_2, w_3, and w_5 spectral regions. The w_1 region (Fig. 2A) showed the lowest discriminant power, indicating the existence of small or undetectable spectral modifications after lethal treatments. The w_2 region (Fig. 2B), with the influence of the functional groups of proteins and peptides, was predominantly affected by acid and heat treatments, whereas alkaline and oxidative lethal stress conditions gave rise to shorter spectral modifications. With regard to the w_3 region (Fig. 2C), the most remarkable spectral changes again were found for *S.* Typhimurium cells treated under acid conditions, while alkaline, heat, and oxidative challenges caused minor spectral modifications. Finally, the HCA of the w_5 spectral region (Fig. 2E) showed that acid stress and alkaline stress originated important changes in FT-IR spectra. Moreover, this region also allowed for a good discrimination between short and long heat treatments. Once again, oxidative stress did not influence the IR spectra obtained.

To correlate spectroscopic data with ultrastructural changes caused by heat, acid, alkaline, or oxidative treatments, transmission electron micrograph data were collected for nontreated and treated samples after a 1-log cycle of inactivation (Fig. 4). Nontreated control samples consisted mostly of single or dividing cells, with a centrally situated genome surrounded by the cytoplasmic area with tightly packed ribosomes. The cell membrane and wall and the periplasmic space of these cells can clearly be distinguished. In accordance with our FT-IR results, oxidative and heat treatments showed small effects on the ultrastructure of *S.* Typhimurium cells, which were limited to the damage of the bacterial membrane, which showed a winding shape, and in the case of oxidative stress-treated cells they looked detached from the cytoplasmic content in some bacteria. On the other hand, bacterial exposure to acidic or alkaline conditions gave rise to a loss of the general cellular shape, with the disorganization of the genome area, appear-

FIG. 1. (A, C, E, G) Survival curves of *Salmonella* Typhimurium CECT 443 after acid (pH 2.5 [A]), alkaline (pH 11.0) (C), heat (55°C) (E), and oxidative (H_2O_2, 40 mM) (G) treatment. The symbols represent the experimental data obtained, while the lines were the result of the adjustment of the data through the mathematical model log $N_t/N_0 = -(t/\delta)^p$. (B, D, H) Untransformed representative FT-IR spectra (1,450 to 800 cm^{-1}) of nonacid-treated cells (black line) and (B) acid-, (D) alkaline-, and (H) oxidative stress-treated cells for 5, 10, 20, 30, and 40 min (all with gray lines). (F) Untransformed representative FT-IR spectra (1,450 to 800 cm^{-1}) of non-heat-treated cells (black line) and heat-treated cells at 55°C for 3, 6, 9, 12, and 15 min (all with gray lines). A, absorbance.

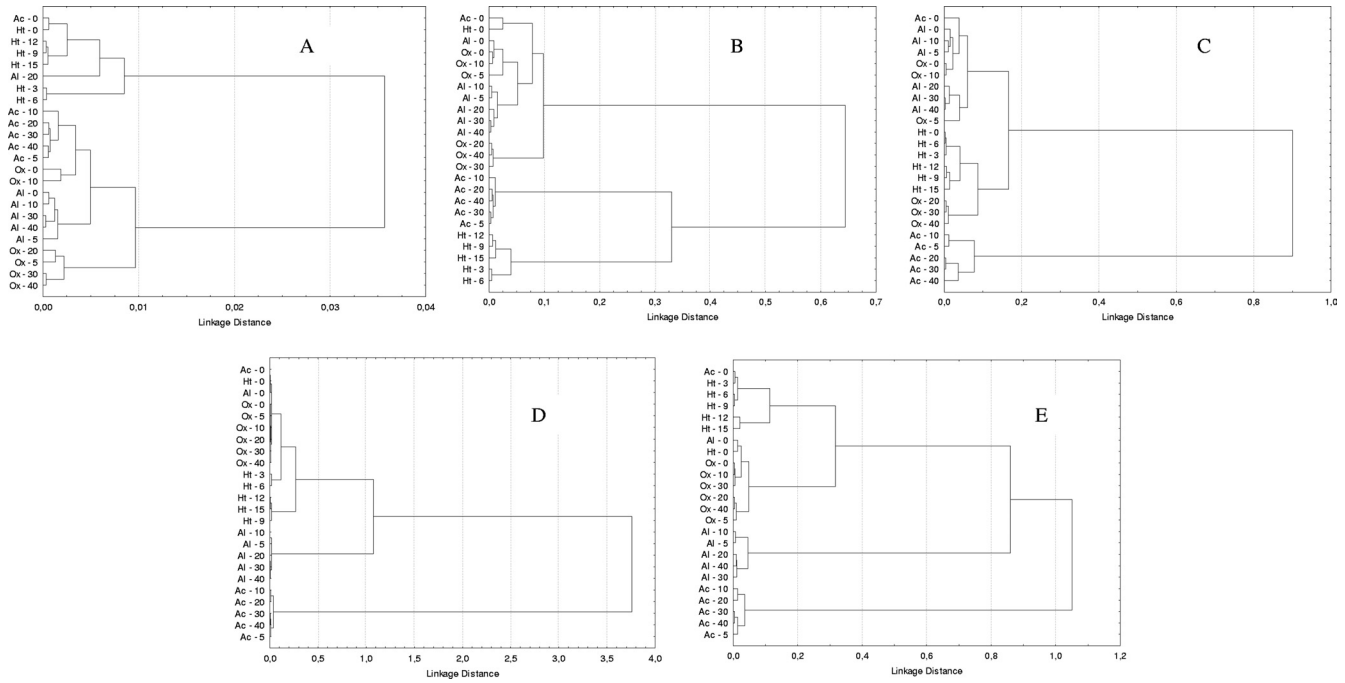

FIG. 2. Dendrograms obtained from w_1 (3,000 to 2,800 cm^{-1}) (A), w_2 (1,800 to 1,500 cm^{-1}) (B), w_3 (1,500 to 1,200 cm^{-1}) (C), w_4 (1,200 to 900 cm-^{1}) (D), and w_5 (900 to 700 cm^{-1}) (E) spectral region data of *S.* Typhimurium nontreated and acid-, alkaline-, heat-, and oxidative stress-treated cells, with cluster analysis performed with the Pearson product moment correlation coefficient and by the Ward algorithm method. Ac − *t*, samples treated at pH 2.5 for *t* min; Al − *t*, samples treated at pH 11.0 for *t* min; Ht − *t*, samples treated at 55°C for *t* min. Ox − *t*, samples treated with H_2O_2 at 40 mM for *t* min.

ance of blank spaces in the cytoplasm, and condensation of the cytoplasmic material toward the membrane, which showed a winding shape and, in some places, seemed disrupted.

The effect of lethal acid, alkaline, heat, and oxidative conditions on *S.* Typhimurium membrane integrity was further assessed by measuring the optical density at 260 nm (OD_{260}) and 280 nm (OD_{280}) of cell-free filtrates from nontreated and treated samples at several points in time (Fig. 5). Although all of the lethal treatments assayed caused a significant increase in both the OD_{260} and OD_{280}, the magnitude of this absorbance increase was dependent on the challenge condition. Thus, whereas acid treatment caused the mildest increase in absorbance, with OD_{260} and OD_{280} values around 2 and 1.5 times higher, respectively, after a 40-min challenge at pH 2.5, a 40-min treatment at pH 11.0, or with H_2O_2 (40 mM) increased these absorbance values around 6 (OD_{260}) and 3 (OD_{280}) times, respectively. On the other hand, heat-treated samples showed the highest values, with OD_{260} and OD_{280} values around 10 and 5 times higher, respectively, after 15 min at 55°C. It is important to note that, in general, OD_{260} and OD_{280} values increased with increasing treatment time, with the exception of oxidative stress exposure, for which these parameters were maximal after 5 min of treatment and slightly decreased with treatment time.

In a search for a physiological explanation for the tailing effect observed for *S.* Typhimurium heat-treated cells, viable cells after a heat treatment at 55°C for 12 min were sorted, and the viable population was isolated and stored under refrigeration until its subsequent use in heat resistance experiments. The original *S.* Typhimurium population (*S.* Typhimurium CECT 443) and the population isolated using the cytometric approach (*S.* Typhimurium CECT 443 v-12) showed similar inactivation kinetics (Fig. 6), with concave upward survival curves and with similar inactivation rates at short treatment times (3 and 6 min). However, at longer treatment times (9, 12, and 15 min), *S.* Typhimurium CECT 443 v-12 showed a slight increase in heat resistance compared to that of *S.* Typhimurium CECT 443, although in most cases no statistically significant differences ($P > 0.05$) were found. The heat resistance of a new bacterial population (*S.* Typhimurium CECT 443 v-12-2) isolated from *S.* Typhimurium CECT 443 v-12 cells also was evaluated (Fig. 6). However, no further increase in heat resistance was detected.

DISCUSSION

FT-IR spectroscopy is a physicochemical method that can determine the global chemical features of cells, and therefore it represents an adequate technique to study the molecular changes after stress exposure, since significant changes in the chemical composition of cells previously have been described in response to a wide variety of stress conditions, including heat, acid, alkaline, and oxidative stress (14, 30, 33, 36). Thus, the FT-IR spectroscopic data collected from bacterial cells exposed to heat, acid, alkaline, and oxidative lethal stress conditions may contribute to improving our understanding of the molecular aspects of the bacterial response to those adverse conditions. In addition, FT-IR spectroscopy also may have applications for detecting stress-injured and dead bacterial cells and for discriminating between different treatment tech-

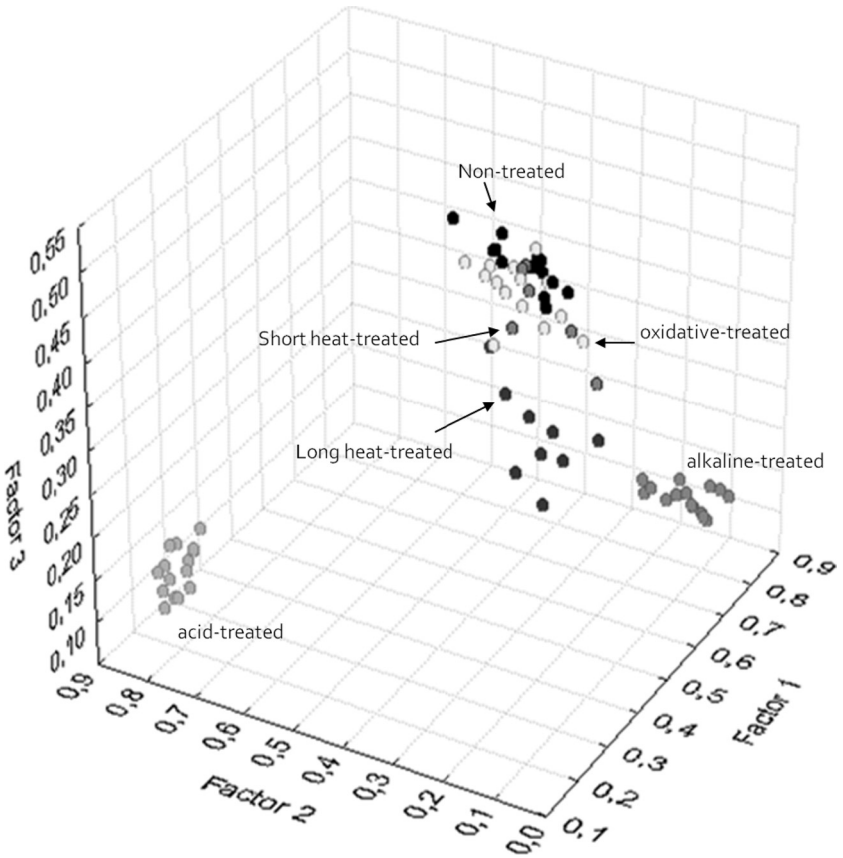

FIG. 3. Scatter plot obtained from factor analysis of the w_4 (1,200 to 900 cm^{-1}) spectral region, showing in gray scale the distribution of nontreated samples and acid-treated, alkaline, short-time heat-treated (3 and 6 min at 55°C), long-time heat-treated (9, 12, and 15 min at 55°C), and oxidative stress-treated samples. Three replicates of each experimental condition are represented.

nologies and treatment intensities (2). However, little research effort has been made to assess the variability of bacterial IR spectrum after exposure to different stress environments. With regard to *S.* Typhimurium, its FT-IR spectrum under stress conditions has been determined previously (2) using heat-treated cells. In the present study we have shown that FT-IR spectra of *S.* Typhimurium cells are greatly affected by the bacterial exposition to lethal stress conditions, and that the changes observed are dependent on the stress condition tested. To this aim, *S.* Typhimurium cells were treated (i) at 55°C, (ii) with pH 2.5, (iii) with pH 11.0, and (iv) with H_2O_2 (40 mM), and their survival and FT-IR spectroscopic profiles were analyzed at different treatment times. The survival curves and the inactivation parameters obtained were similar to those previously described in the literature for this microorganism (3, 4, 5, 6, 15), with the exception of heat treatment, which rendered survival curves concave upward, in contrast to the linear curves previously observed in our laboratory at several heating temperatures using BHI or fruit juices as the heating medium (3, 5). It is important to note that in the present study PBS was used as the heating medium, and this could be responsible for the different behaviors observed. The exact nature of the tailing effect described here is not exactly known, but it could be explained by two different possibilities: (i) the existence of two subpopulations with different constitutive heat resistance, and (ii) the development of a gradual adaptive response that results in an enhancement in heat resistance with increasing treatment time. With regard to the FT-IR spectroscopic data, the HCA and FA showed that the treatment of *S.* Typhimurium cells under lethal heat, acid, and alkaline conditions causes important modifications in the five characteristic spectral regions (w_1, w_2, w_3, w_4, and w_5), which indicates that some or all of the cell compounds, like polysaccharides of the cell wall, fatty acids of the cell membrane, proteins, nucleic acids, or other compounds of the cell that may absorb in these spectral regions, undergo significant alterations during these inactivation treatments. On the other hand, oxidative stress did not significantly affect the IR spectrum observed, which does not indicate the absence of a defensive bacterial response to this stressful agent. Nevertheless, each treatment condition caused specific effects on the different spectral ranges. *S.* Typhimurium exposure to lethal acid, alkaline, heat, and oxidative environments gave rise to minor effects on the w_1 spectral region, which indicates the occurrence of small or undetectable alterations on membrane fatty acids. Acid and heat stress were the stress conditions that modified the w_2 spectral range to a higher extent, probably due to protein denaturation during the treatment. The greatest changes in the w_3 spectral region also were found for *S.* Typhimurium acid-treated cells. Acid treatment mainly affected the band at approximately 1,400 cm^{-1} due to the superposition of C-O-H in plane bending (1,415 cm^{-1}) and $C(CH_3)_2$ stretching (1,402 cm^{-1}). Carbohydrates, the DNA/

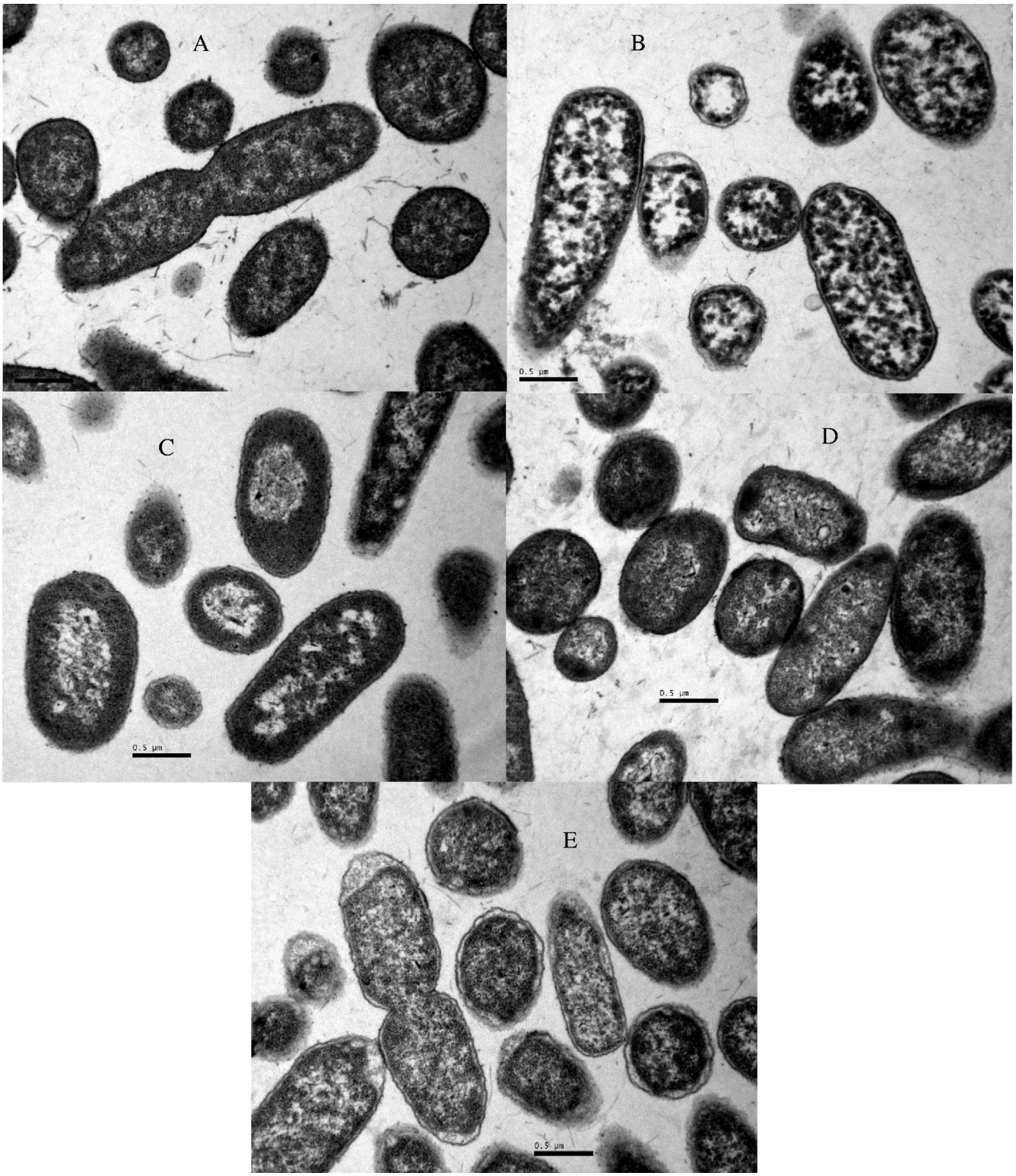

FIG. 4. Electron micrograph sections of *S.* Typhimurium CECT 443 cells. (A) Nontreated cells; (B) acid-treated cells (1 $\log_{10}$ cycle reduction at pH 2.5); (C) alkaline-treated cells (1 $\log_{10}$ cycle reduction at pH 11.0); (D) heat-treated cells (1 $\log_{10}$ cycle reduction at 55°C); and (E) oxidative stress-treated cells (1 $\log_{10}$ cycle reduction at H_2O_2 at 40 mM).

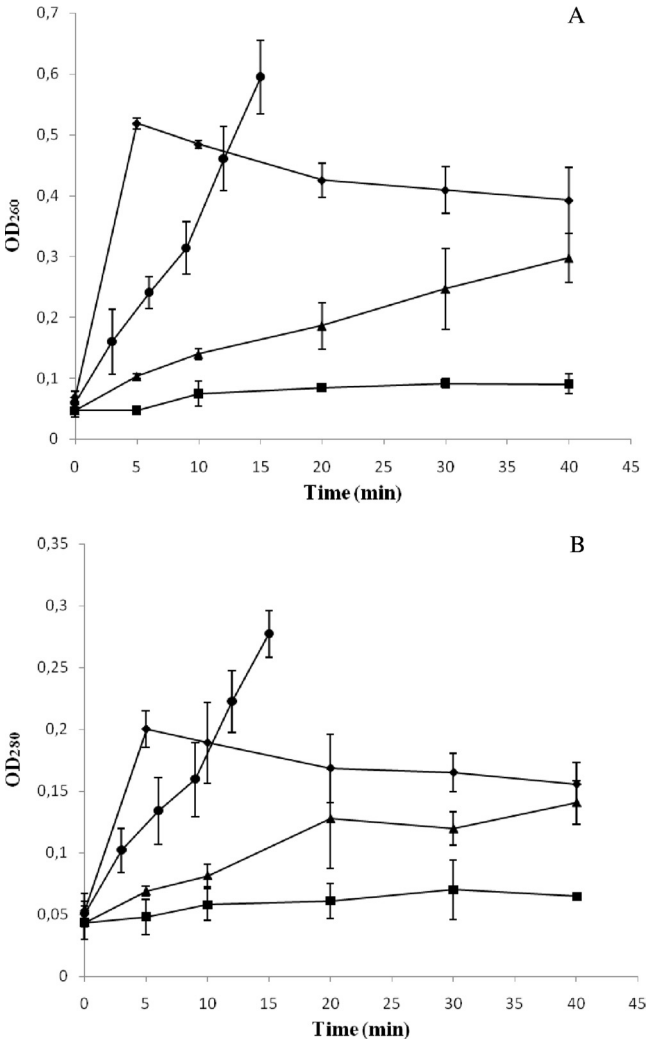

FIG. 5. Increase in OD_{260} (A) and OD_{280} (B) of cell-free filtrates of *S.* Typhimurium CECT 443 cultures after acid (■), alkaline (▲), heat (●), and oxidative (◆) treatment.

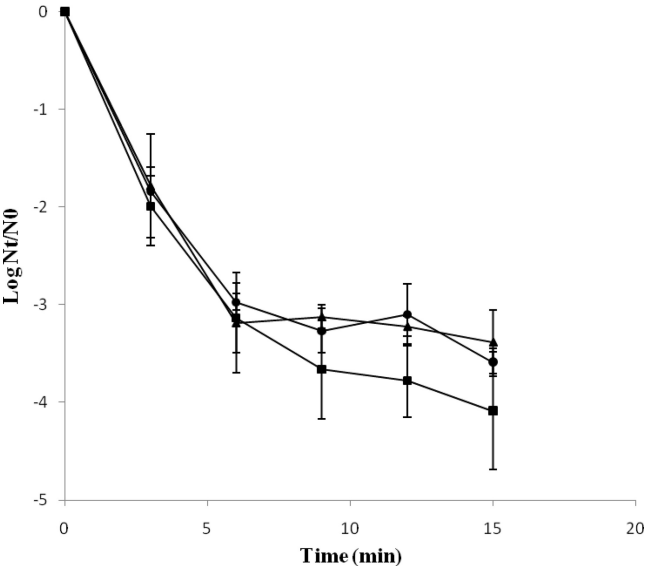

FIG. 6. Survival curves of *S.* Typhimurium CECT 443 (■), *S.* Typhimurium CECT 443 v-12 (▲), and *S.* Typhimurium CECT 443 v-12-2 (●) treated at 55°C in PBS.

RNA backbone, and proteins all contribute to this band (36). Some remarkable differences, even in the absence of any spectral transformation, were found in the w_4 spectral region, which could suggest that part of the IR changes were due to the presence of damage or conformational/compositional alterations in some or all of the components of the cell wall and cell membrane. An FA of this spectral region showed that alkalinization and, especially, acidification were the stress conditions that exerted a stronger effect on the FT-IR spectroscopic profiles, indicating a higher degree of membrane/wall damage or chemical modification after bacterial exposition to them. Nevertheless, it is important to bear in mind that although the w_4 spectral region is dominated by the ring vibrations of the functional groups C-O-C and C-O from the carbohydrates of the cell wall in the range of 1,200 to 1,000 cm^{-1}, where the main changes linked to acid treatments occur, other functional groups, such as the δ(COP), δ(CC), and δ(COH) groups, which represent the contribution due to the DNA and RNA backbone (~1,160 cm^{-1}), the ν(P=O) group from nucleic acids and phospholipids (1,085 cm^{-1}), and the ν(CC) group from DNA and RNA molecules (1,076 cm^{-1}), contribute to the FT-IR profile at this spectral region (36). With regard to the w_5 spectral range, where absorbance is due mostly to the C=C and N=C groups in nucleotides (900 to 800 cm^{-1}), alkaline treatment, with visible changes in the range 915 to 858 cm^{-1}, caused the most important spectral changes, although acid exposure also significantly modified the spectra recorded.

Although several studies have been carried out to elucidate the molecular and physiological changes associated with *Salmonella* sp. response to heat, acid, alkaline, and oxidative stress, the mechanisms involved are not completely understood, although information available in the literature suggests the existence of a complex bacterial response with the implication of several defense strategies, such as the induction of pH homeostatic systems (6, 30), the synthesis of shock proteins (i.e., acid shock proteins [ASP] and heat shock proteins [HSP]) (14, 37), the activation of antioxidative enzymatic systems (i.e., catalase, alkyl hydroperoxidase, and glutathione reductase) (33), and the induction of modifications in membrane fatty acid composition and membrane/wall properties (3, 32). Evidence provided in this study showing changes in all spectral regions in response to environmental lethal conditions supports the existence of a global and complex bacterial response, even though the changes observed in the FT-IR spectra could be due either to the bacterial response to the stress conditions imposed or to the passive damage caused by the treatments on the cellular structures.

An unexpected finding was that changes in FT-IR spectra generally were obvious after short treatment times and did not progress with the increase in the treatment time/intensity. The heat treatment represented an exception to this behavior. Thus, an FA of the w_4 spectral region allowed us to discriminate between soft treatments (3 and 6 min at 55°C) and strong

treatments (9, 12, and 15 min at 55°C). This fact suggests the existence of a bacterial adaptive response throughout the heating, with clear compositional and conformational changes in several cellular compounds, which results in an enhanced heat resistance as the treatment time increases and, therefore, in the appearance of concave upward survival curves. To verify this hypothesis, viable cells after a 12-min treatment were isolated (*S.* Typhimurium CECT 443 v-12) and their heat resistance was tested (Fig. 6). Survival curves obtained again were concave upward, and this fact suggests the inexistence of two initial subpopulations with different constitutive heat resistance levels, since in that case a first inactivation kinetic would be more likely.

The large spectral modifications observed in the w_4 region suggesting damage or conformational/compositional alterations in cell wall and cell membrane components led us to assess the changes in bacterial ultrastructure and in membrane integrity following a lethal treatment under the different stress conditions tested. The ultrastructural observations were clearly linked to the FT-IR profiles obtained. Thus, the stress conditions that resulted in larger modifications in the IR spectra (acidification and alkalinization) also caused the most prominent ultrastructural changes after a 1-log cycle reduction, with a loss of the general cellular shape, disorganization of the genome area, the appearance of blank spaces in the cytoplasm, and the condensation of the cytoplasmic material toward the membrane, which showed a winding shape and, on some occasions, looked disrupted. These morphological features, which probably indicate the existence of DNA degradation and release and the denaturation and precipitation of proteins and other cellular components, agree with previous observations (16, 31) for *Salmonella* cells treated in alkaline and acid environments, respectively. On the other hand, under all of the stress conditions assayed, an increase in the OD_{260} and OD_{280} of cell-free filtrates was observed, which is indicative of the loss of membrane integrity, since OD_{260} and OD_{280} values vary as a function of the amount of nucleic acids and proteins released from bacterial cells and, therefore, present in cell-free filtrates (31). However, this effect was dependent on the stress condition tested. Thus, whereas heat and oxidative stress seem to compromise the membrane integrity to a large extent, acid and alkaline stress gave rise to a slight increase of OD_{260} and OD_{280} values. Therefore, overall results suggest that whereas heat and oxidative stress cause a larger loss of membrane integrity with larger amounts of released cytoplasmic material, their effect on the physicochemical properties of the cellular envelopes (mainly represented by w_1 and w_4 spectral regions) was minimal. However, significant conformational/compositional changes were observed for acid- and alkaline-treated cells, especially in the w_4 spectral range. It is important to note that the cell envelopes are complex structures comprised by more than just polysaccharides and fatty acids, and therefore other substances, such as proteins, also are responsible for membrane integrity. Thus, the great changes observed in the w_2 spectral region in response to heat treatments could account for the higher loss of membrane integrity linked to this lethal stress exposure. Furthermore, losses of membrane integrity also may be due to subtle changes in conformation that are not detectable, as they are covered by other stronger absorptions.

Evidence provided in this study also shows that the loss of membrane integrity observed for *S.* Typhimurium cells is dependent on the treatment time, except for cells exposed to oxidative stress, which showed a similar degree of membrane damage under the different treatment intensities assayed. Previous results (31) described for *S.* Enteritidis cells that were alkaline treated in the presence of trisodium phosphate reported an increased release of 260-nm-absorbing material to the medium and the presence of DNA, proteins, and lipopolysaccharides in the cell-free filtrates. Our study demonstrates that stress conditions aside from alkalinization also cause membrane damage with the loss of membrane integrity, with this effect being even greater for cells exposed to heat and oxidative stress.

In conclusion, results obtained not only indicate the potential of FT-IR spectroscopy to discriminate between intact and injured bacterial cells and between treatment technologies but also show the capacity of this technique to study the molecular aspects of the bacterial stress response, as confirmed by the concordance of FT-IR data with ultrastructural changes observed by transmission electron microscopy. Spectral changes were maximal for acid and alkaline stress and for the w_4 spectral region, which indicates the existence of alterations in membrane and wall conformation/composition after acid and alkaline treatments. The IR and transmission electron micrograph data together suggest the existence of a complex bacterial stress response where modifications in substances like polysaccharides of the cell wall, fatty acids of the cell membrane, proteins, and nucleic acids are involved, even though the changes observed in the FT-IR spectra could be due either to the active bacterial response to the stress conditions imposed or to the passive damage caused by the treatments on the cellular structures. Clear evidence for the induction of membrane damage or alterations in membrane compositions after heat, acid, alkaline, and oxidative treatments has been found.

ACKNOWLEDGMENT

We acknowledge the financial contribution of the Spanish Ministry of Science and Innovation (Plan Nacional I+D+I, Ref. AGL2008-02668).

REFERENCES

1. **Al-Qadiri, H. M., M. Lin, A. G. Cavinato, and B. A. Rasco.** 2006. Fourier transform infrared spectroscopy, detection and identification of *Escherichia coli* O157:H7 and *Alicyclobacillus* strains in apple juice. Int. J. Food Microbiol. **111:**73–80.
2. **Al-Qadiri, H. M., M. Lin, M. A. Al-Holy, A. G. Cavinato, and B. A. Rasco.** 2008. Detection of sublethal termal injury in *Salmonella enterica* serotype Typhimurium and *Listeria monocytogenes* using Fourier transform infrared (FT-IR) spectroscopy (4000 to 600 cm^{-1}). J. Food Sci. **73:**54–61.
3. **Alvarez-Ordóñez, A., A. Fernández, M. López, R. Arenas, and A. Bernardo.** 2008. Modifications in membrane fatty acid composition of *Salmonella typhimurium* in response to growth conditions and their effect on heat resistance. Int. J. Food Microbiol. **123:**212–219.
4. **Álvarez-Ordóñez, A., A. Fernández, A. Bernardo, and M. López.** 2009. Comparison of acids on the induction of an acid tolerance response in *Salmonella* Typhimurium, consequences for food safety. Meat Sci. **81:**65–70.
5. **Alvarez-Ordóñez, A., A. Fernández, A. Bernardo, and M. López.** 2009. A comparative study of thermal and acid inactivation kinetics in fruit juices of *Salmonella enterica* serovar Typhimurium and *Salmonella enterica* serovar Senftenberg grown at acidic conditions. Foodborne Pathog. Dis. **6:**1147–1155.
6. **Alvarez-Ordóñez, A., A. Fernández, A. Bernardo, and M. López.** 2010. Arginine and lysine decarboxylases and the acid tolerance response of *Salmonella* Typhimurium. Int. J. Food Microbiol. **136:**278–282.
7. **Alvarez-Ordóñez, A., J. Halisch, and M. Prieto.** 2010. Changes in Fourier transform infrared spectra of *Salmonella enterica* serovars Typhimurium and

Enteritidis after adaptation to stressful growth conditions. Int. J. Food Microbiol. **142:**97–105.
8. **Amiali, N. M., M. R. Mulvey, J. Sedman, M. Louie, A. E. Simor, and A. A. Ismael.** 2007. Rapid identification of coagulase-negative staphylococci by Fourier transform infrared spectroscopy. J. Microbiol. Methods **68:**236–242.
9. **Baldauf, N. A., L. A. Rodríguez-Romo, A. Männig, A. E. Yousef, and L. E. Rodríguez-Saona.** 2007. Effect of selective growth media on the differentiation of *Salmonella enterica* serovars by Fourier-transform mid-infrared spectroscopy. J. Microbiol. Methods **68:**106–114.
10. **Curk, M. C., F. Peladan, and J. C. Hubert.** 1994. Fourier transform infrared (FT-IR) spectroscopy for identifying *Lactobacillus* species. FEMS Microbiol. Lett. **123:**241–248.
11. **D'Aoust, J. Y.** 2000. *Salmonella*, p. 1233–1299. *In* B. M. Lund, T. C. Baird-Parker, and G. W. Gould (ed.), The microbiological safety and quality of foods. Aspen, Gaithersburg, MD.
12. **Ede, S. M., L. M. Hafner, and P. M. Fredericks.** 2004. Structural changes in the cells of some bacteria during population growth: a Fourier transform infrared-attenuated total reflectance study. Appl. Spectrosc. **58:**317–322.
13. **European Food Safety Authority.** 2010. The community summary report on trends and sources of zoonoses, zoonotic agents and food-borne outbreaks in the European Union in 2008. EFSA J. doi:10.2903/j.efsa.2010.1496.
14. **Foster, J. W.** 2000. Microbial responses to acid stress, p. 99–115. *In* G. Storz and R. Hengge-Aronis, (ed.), Bacterial stress responses. ASM Press, Washington, DC.
15. **Greenacre, E. J., S. Lucchini, J. C. D. Hinton, and T. F. Brocklehurst.** 2006. The lactic acid-induced acid tolerance response in *Salmonella enterica* serovar Typhimurium induces sensitivity to hydrogen peroxide. Appl. Environ. Microbiol. **72:**5623–5625.
16. **Jung, Y. J., K. J. Min, and K. S. Yoon.** 2009. Responses of acid-stressed *Salmonella* Typhimurium in broth and chicken patties to subsequent antimicrobial stress with ε-polylysine and combined potassium lactate and sodium diacetate. Food Microbiol. **26:**467–474.
17. **Kim, S., B. L. Reuhs, and L. J. Mauer.** 2005. Use of Fourier transform infrared spectra of crude bacterial lipopolysaccharides and chemometrics for differentiation of *Salmonella enterica* serotypes. J. Appl. Microbiol. **99:**411–417.
18. **Kuhm, A. E., D. Suter, R. Felleisen, and J. Rau.** 2009. Identification of *Yersinia enterocolitica* at the species and subspecies levels by Fourier transform infrared spectroscopy. Appl. Environ. Microbiol. **75:**5809–5813.
19. **Lamprell, H., G. Mazerolles, A. Kodjo, J. F. Chamba, Y. Noel, and E. Beuvier.** 2006. Discrimination of *Staphylococcus aureus* strains from different species of *Staphylococcus* using Fourier transform infrared (FTIR) spectroscopy. Int. J. Food Microbiol. **108:**125–129.
20. **Lin, M., M. Al-Holy, H. Al-Qadiri, D. H. Kang, A. G. Cavinato, Y. Huang, and B. A. Rasco.** 2004. Discrimination of intact and injured *Listeria monocytogenes* by Fourier transform infrared spectroscopy and principal component analysis. J. Agric. Food Chem. **52:**5769–5772.
21. **Mafart, P., O. Couvert, S. Gaillard, and I. Leguerinel.** 2002. On calculating sterility in thermal preservation methods: application of the Weibull frequency distribution model. Int. J. Food Microbiol. **72:**107–113.
22. **Maradona, M. P.** 1996. Software for microbial fingerprinting by means of the Infrared spectra. Comp. Appl. Biosci. **12:**353–356.
23. **Miguel Gómez, M. A., M. A. Bratos Pérez, F. J. Martín Gil, A. Dueñas Diez, J. F. Martín Rodríguez, P. Gutiérrez Rodríguez, A. Orduna Domingo, and A. Rodríguez Torres.** 2003. Identification of species of *Brucella* using Fourier transform infrared spectroscopy. J. Microbiol. Methods **55:**121–131.
24. **Mouwen, D. J. M., M. J. B. M. Weijtens, R. Capita, C. Alonso-Calleja, and M. Prieto.** 2005. Discrimination of enterobacterial repetitive intergenic consensus PCR types of *Campylobacter coli* and *Campylobacter jejuni* by Fourier transform infrared spectroscopy. Appl. Environ. Microbiol. **71:**4318–4324.
25. **Mouwen, D. J. M., R. Capita, C. Alonso-Calleja, J. Prieto-Gómez, and M. Prieto.** 2006. Artificial neural network based identification of *Campylobacter* species by Fourier transform infrared spectroscopy. J. Microbiol. Methods **67:**131–140.
26. **Naumann, D.** 2000. Infrared spectroscopy in microbiology, p. 102–131. *In* R. A. Meyers (ed.), Encyclopedia of analytical chemistry. John Wiley & Sons Ltd., Chichester, United Kingdom.
27. **Oust, A., T. Moretro, C. Kirschner, J. A. Narvhus, and A. Kohler.** 2004. FT-IR spectroscopy for identification of closely related lactobacilli. J. Microbiol. Methods **59:**149–162.
28. **Oust, A., T. Moretro, K. Naterstad, G. D. Sockalingum, I. Adt, M. Manfait, and A. Kohler.** 2006. Fourier transform infrared and Raman spectroscopy for characterization of *Listeria monocytogenes* strains. Appl. Environ. Microbiol. **72:**228–232.
29. **Rebuffo-Scheer, C. A., J. Schmitt, and S. Scherer.** 2007. Differentiation of *Listeria monocytogenes* serovars by using artificial neural network analysis of Fourier-transformed infrared spectra. Appl. Environ. Microbiol. **73:**1036–1040.
30. **Saito, H., and H. Kobayashi.** 2003. Bacterial responses to alkaline stress. Sci. Prog. **86:**271–282.
31. **Sampathkumar, B., G. G. Khachatourians, and D. R. Korber.** 2003. High pH during trisodium phosphate treatment causes membrane damage and destruction of *Salmonella enterica* serovar Enteritidis. Appl. Environ. Microbiol. **69:**122–129.
32. **Sampathkumar, B., G. G. Khachatourians, and D. R. Korber.** 2004. Treatment of *Salmonella enterica* serovar Enteritidis with a sublethal concentration of trisodium phosphate or alkaline pH induces thermotolerance. Appl. Environ. Microbiol. **70:**4613–4620.
33. **Storz, G., and M. Zheng.** 2000. Oxidative stress, p. 47–59. *In* G. Storz and R. Hengge-Aronis (ed.), Bacterial stress responses. ASM Press, Washington, DC.
34. **van Boekel, M. A. J. S.** 2002. On the use of the Weibull model to describe thermal inactivation of microbial vegetative cells. Int. J. Food Microbiol. **74:**139–159.
35. **Winder, C. L., E. Carr, R. Goodacre, and R. Seviour.** 2004. The rapid identification of *Acinetobacter* species using Fourier transform infrared spectroscopy. J. Appl. Microbiol. **96:**328–339.
36. **Yu, C., and J. Irudayaraj.** 2005. Spectroscopic characterization of microorganisms by Fourier transform infrared microspectroscopy. Biopolymers **77:** 368–377.
37. **Yura, T., M. Kanemori, and M. Y. Morita.** 2000. The heat shock response: regulation and function, p. 3–18. *In* G. Storz and R. Hengge-Aronis (ed.), Bacterial stress responses. ASM Press, Washington, DC.